ACS APPLIED MATERIALS & INTERFACES

Research Article

www.acsami.org

Direct Electrochemical DNA Detection Originated from the Self-Redox Signal of Sulfonated Polyaniline Enhanced by Graphene Oxide in Neutral Solution

Tao Yang,* Le Meng, Xinxing Wang, Longlong Wang, and Kui Jiao

Key Laboratory of Eco-chemical Engineering (Ministry of Education), College of Chemistry and Molecular Engineering, Qingdao University of Science and Technology, Qingdao 266042, China

ABSTRACT: In this paper, a type of direct DNA impedance detection using the self-redox signal change of sulfonated polyaniline (SPAN) enhanced by graphene oxide (GNO) was reported, here SPAN is a copolymer obtained from aniline and *m*-aminobenzenesulfonic acid. The resulting nanocomposite was characterized by scanning electron microscopy, transmission electron microscopy, Fourier transform infrared spectroscopy, cyclic voltammetry, and electrochemical impedance spectroscopy. The $\pi-\pi$ planar structure of GNO and the carboxyl groups on the surface of GNO ensured it could act as an excellent substrate for adsorption and polymerization of aniline monomer. Because of the existence of GNO, the electrochemical activities of SPAN were enhanced obviously. Because of abundant sulfonic acid groups, the resulting nanocomposite showed obvious self-redox signal even at physiological pH, which is beneficial for biosensing field. DNA probes with amine groups could be covalently attached to the modified electrode surface through the acyl chloride cross-linking reaction of sulfonic groups and amines. When the flexible probe DNA was successfully grafted, the electrode was coated and electron transfer between electrode and buffer was restrained. Thus, the inner impedance value of SPAN (rather than using outer classic EIS probe, $[Fe(CN)_6]^{3-/4-}$) increased significantly. After hybridization, the rigid helix opened the electron channel, which induced impedance value decreased dramatically. As an initial application of this system, the PML/RARA fusion gene sequence formed from promyelocytic leukemia (PML) and retinoic acid receptor alpha (RARA) was successfully detected.

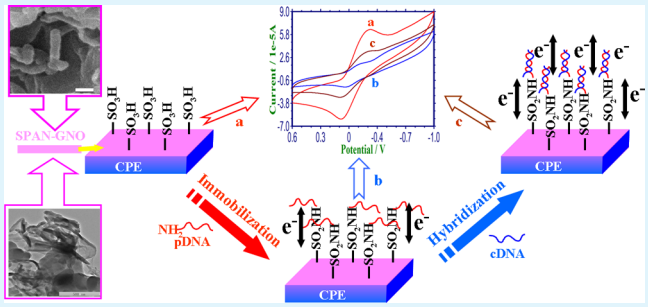

KEYWORDS: *sulfonated polyaniline, graphene oxide, direct electrochemical detection, electrochemical impedance spectroscopy, self-redox signal*

INTRODUCTION

Recently, flourishing researches of electrode materials have emerged, especially novel carbon nanostructures. Among them, graphene shows many advantages such as high surface area with excellent conductivity and low production cost, which induced mass production.[1] Because of its encouraging characteristics, graphene has played a key role in pursuing multifunctional graphene-based composites.[2] Various functional graphene composites by chemical modifications or non-covalent functionalizes have been reported.[3] Among them, polyaniline (PANI) has been adopted to fabricate composites with graphene including doping graphene with pre-obtained PANI; in situ-polymerization of aniline with graphene oxide (GNO) or reduced graphene oxide as dopant, and others. For instance, Wan et al. proposed that the $\pi-\pi$ planar structure of GNO and the carboxyl groups on the surface of GNO could be served as the template and dopant, respectively, to get the PANI with layered structures.[4] Through rapid mixture polymerization of aniline on the surfaces of GNO and graphene papers, respectively, Yan et al. obtained free-standing GNO-PANI and graphene-PANI hybrid papers. Compared with the parent GNO and graphene papers, electrochemical properties of the hybrid papers was remarkably enhanced because of the existence of PANI.[5] Wang et al. also found that less amount of graphene oxide (existed in PANI) could greatly prompt the electrochemical performance of PANI.[6] Through layer-by-layer assembly of sulfonic acid-grafted reduced graphene oxide and polyaniline, enhanced electrical and ionic conductivities, and electrochromic properties were observed, which were attributed to the graphitic structure of the sulfonic acid-grafted reduced graphene oxide sheets and the sulfonic acid groups attached to it.[7] Sulfonated polyaniline (SPAN) has been successfully adopted in the noncovalent functionalization of graphene. Sulfonated polyaniline endows the composite with high conductivity, good electrocatalytic activity, and stability.[8]

DNA sequence detection is very important in numerous human health areas such as diagnostics, genomics, and clinical medicine. Compared with a lot of optical, acoustic, gravimetric, and electronic approaches, electrochemical DNA biosensors have woken significant attention with the advantages such as

Received: July 29, 2013
Accepted: October 2, 2013
Published: October 2, 2013

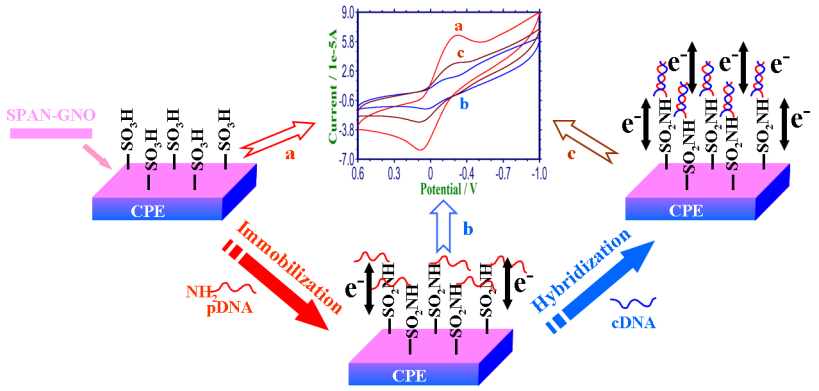

Figure 1. Schematic diagram of the DNA detection on the SPAN-GNO: (a) SPAN-GNO/CPE, (b) ssDNA/SPAN-GNO/CPE, (c) dsDNA/SPAN-GNO/CPE.

simplicity, reliability, portability, sensitivity, and selectivity, etc. Some of electrochemical strategies for DNA sequence detection need a label attached to the DNA target to improve detection limit, but accompanied with faults of poor labeling efficiency, complicated multistep analysis and contamination to samples.[9,10] So label-free, unscathed, and direct electrochemical detection of DNA hybridization has received wide interest. To pursue the signal-amplifying principle, researchers have extensively used various nanomaterials such as GaN nanowires,[11] praseodymium oxide nanoparticles,[12] and polymer nanomaterials[9,13] to construct a direct DNA biosensing platform. Among traditional conducting polymers, polypyrrole,[14] naphthoquinone,[15,16] and polyaniline-based[17,18] materials have been adopted in direct DNA detection. However, one of the main shortcomings of these traditional polymers (such as polyaniline) is toxic and their electrochemical activities are limited in acidic environment or specific electrolyte. Those shortcomings press their application in bioelectrochemistry. It is worth noting that sulfonated PANI owns the good solubility, excellent electrochemical activities, and electrocatalytic ability in neutral solutions even in alkaline solutions.[19−23] Our group has developed an indicator-free impedance assay of DNA hybridization based on highly conductive poly(*m*-aminobenzenesulfonic acid) (PABSA)/TiO_2 nanosheets obtained from the pulse potentiostatic method (PPM).[22] In a neutral environment (phosphate buffer solution, PBS, pH 7.0), the PABSA/TiO_2 nanosheets showed good redox activity and electroconductivity, which could realize direct electrochemical DNA hybridization detection.[22] Besides, as a star nanomaterial, graphene oxide could serve as an ideal platform for one-step electrosynthesis of the poly(*m*-aminobenzenesulfonic acid) and reduced graphene oxide nanocomposite (PABSA-rGNO). The $\pi-\pi$ interaction and hydrogen bonding between the GNO layers and aromatic rings monomer (*m*-aminobenzenesulfonic acid, ABSA) promoted efficient polymerization, the film-forming ability and the water resistance of PABSA-rGNO.[23] The PABSA-rGNO also owned excellent electrochemical activity and thermal stability even in neutral environment, which indicated self-signal change could serve as a powerful tool for direct and freely switchable detection of different target genes.[23]

In this paper, a kind of nanocomposite via a simple and economical chemical synthesis was obtained. The nanocomposite integrated graphene oxide with sulfonated polyaniline, where graphene oxide is a single-atom thick, two-dimensional sheet of sp^2-bonded conjugated carbon and sulfonated polyaniline owns rich-conjugated structures, functional groups, and excellent electrochemical activity. The synergistic interaction of SPAN-GNO nanocomposite resulted in high electrochemical activity in neutral solution (Figure 1, curve a), which could be adopted to construct a direct, electrochemical self-signal amplifying DNA hybridization assay. When the probe DNA was covalently immobilized on the SPAN-GNO layer, the redox peaks of SPAN-GNO almost became nearly invisible ("signal-off", Figure 1, curve b). When hybridization happened, a "signal-on" mode of self-signal (Figure 1, curve c) was observed. The immobilization and hybridization event could change the interfacial properties, such as interfacial electron-transfer resistance and the capacitance.[22] These changes could be observed by the highly sensitive electrochemical impedance spectroscopy (EIS) technology for the target gene detection. To the best of our knowledge, the GNO-enhanced SPAN serving as the sensing platform for the direct electrochemical detection of DNA via self-signal changes has not yet been reported.

EXPERIMENTAL SECTION

Apparatus and Reagents. A CHI 760D electrochemical system (Shanghai CH Instrument Company, China) was applied for the electrochemical data measurement, which was in connection with a carbon paste electrode (CPE) or modified electrodes as working electrode, a saturated calomel as reference electrode (SCE) and a platinum wire as auxiliary electrode. The pH values of all solutions were collected by a model pHS-25 digital acidimeter (Shanghai Leici Factory, Shanghai, China). The resulting composites were characterized by scanning electron microscopy (SEM, JSM-6700F machine, JEOL, Tokyo, Japan), transmission electron microscopy (TEM, JEM 2100 transmission electron microscopy), and Fourier transform infrared spectroscopy (FT-IR) spectrum (Tensor 27 FT-IR spectrophotometer, Bruker Company, Germany).

Carbon powder and Paraffin were purchased from Shanghai Colloid Laboratory and Shanghai Hua Ling Healing Appliance Factory, respectively. Natural graphite (spectral pure, about 30 μm) was obtained from Sinopharm Chemical Reagent Co., Ltd.. Aniline and *m*-aminobenzenesulfonic acid (purity >98.0%) were respectively acquired from Tianjin Da Mao Chemical Factory and Fluka (USA). Tris(hydroxymethyl) amminomethane (Tris) was acquired from Sigma (St. Louis, MO, USA). Sodium dodecyl sulfate (SDS) was purchased from Shanghai Reagent Company (Shanghai, China) and used as received.[23] All the chemicals were of analytical grade and aqueous solutions were prepared with Aquapro ultrapure water system (Ever Young Enterprises Development. Co. Ltd., Chongqing, China).

The 18-base synthetic oligonucleotides probe (pDNA), its complementary DNA (cDNA, target DNA, namely a 18-base fragment of PML/RARA fusion gene sequence formed from promyelocytic

leukemia (PML) and retinoic acid receptor alpha (RARA)), single-base mismatched DNA, and non-complementary DNA (ncDNA) were synthesized by Shanghai Sangon Biotechnology Co. Ltd. (Shanghai, China). Their base sequences and stock solutions were same as reference.[23,24]

Preparation of Modified Electrodes. The preparation of CPE was based on the method reported by Yang.[23] Graphite oxide (GO) was prepared from graphite powder according to a modified Hummers method.[25] GNO was obtained after the resulting GO suspending in water and sonicating for 30 min. Sulfonated polyaniline-graphene oxide (SPAN-GNO) nanocomposite was synthesized by adding a known amount of aniline (ANI), *m*-aminobenzenesulfonic acid (ABSA), GNO, and ammonium persulfate (APS) to the aqueous suspension; stirring; and allowing reaction for a given time at 4 °C.[26] The aqueous suspension was then filtered and washed with ultrapure water until the filtrate became neutral, and naturally dried in the air. For comparison, polyaniline-graphene oxide (PANI-GNO) hybrid, and poly(*m*-aminobenzenesulfonic acid)-graphene oxide (PABSA-GNO) hybrid were carried out using the similar procedure.

The resulting hybrids were respectively suspended in water to obtain a homogeneous dispersion and then sonicated for a given time to get aqueous suspensions. Twenty microliters of hybrid suspension were dripped onto the fresh surface of CPE and then dried naturally in the air to form modified electrodes. These obtained electrodes were denoted as SPAN-GNO/CPE, PANI-GNO/CPE, and PABSA-GNO/CPE, respectively. In addition, 20 μL of 1.0 mg/mL GNO suspension was coated on CPE uniformly to obtain the GNO/CPE. SPAN/CPE was prepared under the same condition using CPE as working electrode but without GNO.

Immobilization and Hybridization..[22,23] On the basis of the covalent bonding between the amine group of the DNA probes and the sulfonic acid groups of the SPAN-GNO film,[27] pDNA could be immobilized on the SPAN-GNO/CPE surface, denoted as pDNA/SPAN-GNO/CPE, shown in Figure 1b. Firstly, the modified electrode was immersed in an acetone solution containing PCl_5 (40 mmol/L) for a given time to activate the sulfonic acid groups of the SPAN-GNO film. After activating, the modified electrode was rinsed with Tris-HCl (pH 7.0) buffer solution to wash off the excess PCl_5.[22] A 20.0 μL Tris-HCl (pH 7.0) buffer solution containing 1.0×10^{-7} mol/L pDNA was pipetted onto the modified electrode and air-dried to dryness, rinsed with ultrapure water to remove the unimmobilized pDNA. The hybridization reaction was realized by transferring 2× sodium saline citrate (2× SSC) buffer solution (20.0 μL) containing a series of cDNA solution onto the pDNA/SPAN-GNO/CPE and air-dried (about 2 h). To remove the unhybridized cDNA, the electrode was washed with 0.2% SDS solution. The same procedure as mentioned above was applied to the pDNA/SPAN-GNO/CPE for hybridization with single-base mismatched and non-complementary sequences.[23]

Electrochemical Measurements. Cyclic voltammogram (CV) measurements were carried out in 0.3 mol/L PBS (pH 7.0) between −-1.0 V and 1.2 V at a scan rate of 0.1 V/s.

EIS measurements were also carried out in 0.3 mol/L PBS (pH 7.0).[23] The AC voltage amplitude was 5 mV and the voltage frequencies ranged from 0.1 Hz to 1×10^4 Hz under open-circuit potential.

RESULTS AND DISCUSSION

Characterization of Hybrid. The SEM images of GNO, SPAN, and SPAN-GNO are shown in Figure 2A-C. From Figure 2A, it can be seen that GNO nanosheets presents smooth platform with slight wrinkles.[28] The SPAN nanofibres (Figure 2B) are interconnected together to present net-like nanostructures. The SPAN nanofibres are very uniform with the length up to several micrometers and with 40-70 nm in diameter. From Figure 2C, three dimensional interconnected GNO with intercalated SPAN is clearly observed. Meanwhile, the intercalation between SPAN and GNO also can be proved by TEM image (Figure 2D), where the SPAN-GNO nanocomposite presents the SPAN nanofibers are coated by transparent, paperlike GNO. The formed homologous structure of the composite film maybe originated from the GNO, which served as a support material (because of $\pi-\pi$ interaction between SPAN and GNO)[23] and offered a large number of active sites for nucleation growth of SPAN. In addition, it is hard to observe individual GNO or SPAN, which indicates the SPAN and GNO had been integrated successfully.[23] The moderate amount of GNO nanosheets dispersed in the polymer chain structure give a more regular structure, which is beneficial for electron transfer along and among polymer chains.[22] The open and three dimensional interconnected structure of the resulting SPAN-GNO owns a large surface area and provides more activation sites, which could enhance the DNA immobilization amount and insure steric orientation.[22]

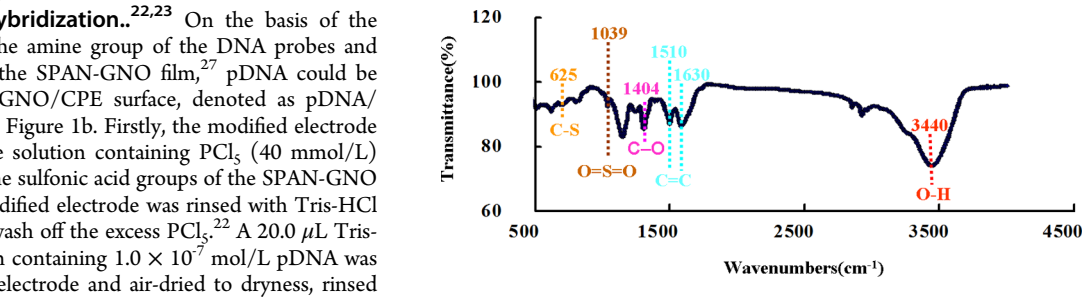

Figure 2. SEM images of (A) GNO, (B) SPAN, (C) SPAN-GNO; and (D) TEM image of SPAN-GNO.

At the same time, the characteristic groups on the composite can be confirmed by the FT-IR data.[23,29] In Figure 3, the

Figure 3. FT-IR spectra of SPAN-GNO.

characteristic peaks of GNO and SPAN are clearly observed in SPAN-GNO composite. The peak at 1630 cm^{-1} corresponds to aromatic C═C and bands at 1404 cm^{-1} to carboxyl C−O group located at the edges of the GNO nanosheets.[23,30] A very broad and intense peak at 3440 cm^{-1} confirms the O−H groups of carboxylic acid on the GNO sheets.[31] The characteristic peaks of SPAN, such as the C═C stretching vibration of quinoid (1510 cm^{-1}),[31] the O═S═O stretching vibration (1039 cm^{-1}), and C−S stretching vibration (625 cm^{-1}) are observed, respectively.[29] On the basis of all of the above peaks, it can be seen that the GNO and SPAN have been effectively integrated to form the SPAN-GNO composite.

Cyclic Voltammetry of Different Modified Electrodes. Figure 4 shows the redox signals of the various electrodes, which were investigated by the CV technique in 0.3 mol/L PBS (pH 7.0). Compared with the signals of GNO/CPE (panel A), SPAN/CPE (panel B) shows a well-defined redox peaks. For SPAN-GNO/CPE (panel C), the dramatically increased redox peak currents are observed in comparison with the other modified electrodes. These enhanced currents could be attributed to the addition of graphene oxide into SPAN, which obviously improve the self-redox activity of SPAN. The results further confirmed that the open and ramified morphology[22] of the SPAN-GNO layers (Figure 2C) is

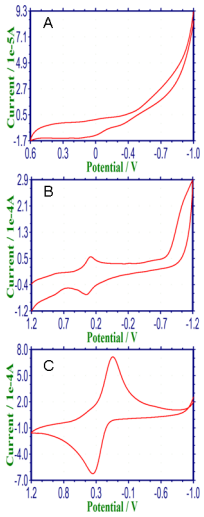

Figure 4. The CVs of GNO/CPE (A), SPAN/CPE (B), and SPAN-GNO/CPE (C) in 0.30 mol/L PBS (pH 7.0).

beneficial for electron transfer of SPAN between supporting buffer and electrode surface.

Optimization of the Fabrication Condition. Herein, the SPAN-GNO hybrid was yielded for a given time. So, the reaction time and the mass ratio of aniline (ANI): ABSA could affect the self-redox activity of SPAN-GNO hybrid.

The CVs of the various SPAN-GNO hybrids, which were produced in different reaction time (such as 5, 8, 13, 18, and 24 h), are shown in Figure 5A. Accompanied with the reaction time prolonged, the peak currents increased. After 18 h, the peak currents decreased, indicating that the optimum reaction time is 18 h.

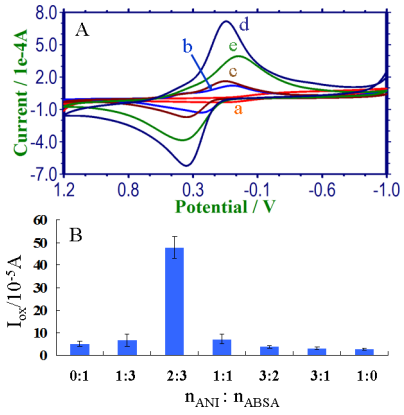

Figure 5. (A) CVs of the SPAN-GNO original from different reaction time in 0.30 mol/L PBS (pH 7.0). The reaction time: (a) 5, (b) 8, (c) 13, (d) 18, and (e) 24 h. (B) Effect of mass ratio of ANI: ABSA (n_{ANI}:n_{ABSA}) on oxidation peak current values of SPAN-GNO nanocomposite.

Just as the statement in the introduction, the electrochemical activities of polyaniline are limited in acidic environment or specific electrolyte, which restrict their application in bioelectrochemistry. Thus, the introduction of sulfonated PANI can help improve electrochemical activities in neutral solutions for direct DNA detection. In this system, SPAN is a copolymer of aniline and *m*-aminobenzenesulfonic acid.[26] For comparison, pure polyaniline-graphene oxide (PANI-GNO), poly(*m*-aminobenzenesulfonic acid)-graphene oxide (PABSA-GNO), and the hybrids obtained from different mass ratios of ANI: ABSA were carried out using the similar procedure. According to the same method above, the effect of different mass ratios of ANI: ABSA was also investigated (Figure 5B). The oxidation peak current values (I_{ox}) were adopted to evaluate the optimum mass ratio of ANI:ABSA.[26,29] The histogram of I_{ox} shows that the optimum mass ratio of ANI:ABSA is 2:3.

On the whole, SPAN-GNO hybrid owns large specific surface area, plenty of electrochemical sites, and high conductivity in 0.3 mol/L PBS (pH 7.0), which ensure it as a highly sensitive electrochemical sensing platform for monitoring the state of electrodes and the further obtained DNA layer.[32,33]

Electrochemical Studies on DNA Immobilization and Hybridization. EIS, as a sensitive and reliable tool, has been widely applied to study the surface property change of electrode interface for biological and chemical molecule recognition.[22,34] The DNA immobilization and hybridization were investigated by the EIS technique in 0.3 mol/L PBS (pH 7.0), and the results are shown in Figure 6A.[23] When the pDNA was covalently bounded to the SPAN-GNO layers, the impedance value increased (curve b) compared with that of the SPAN-GNO (curve a). The pDNA possesses rich negative charges and the flexible characteristics, which can block the effective electron transfer. So the increase of impedance value is a strong evidence that pDNA was successfully immobilized on the SPAl N-GNO layers. After hybridization with the cDNA, an obvious decrease of impedance value is shown in curve c.[35] Conformation could be changed after hybridization, that is flexible single-stranded DNA (ssDNA) often presents as random coils, whereas double-stranded DNA (dsDNA) lead to a helix and rigid surface, which opened the electron channel and induced impedance value decreased dramatically. Therefore, the SPAN-GNO layers could be used to directly monitor the cDNA without any complex labeling steps and outer indicators.

To investigate the selectivity of the DNA detection, we hybridized the probe-modified electrode with different DNA sequences (including single-base mismatched and non-complementary sequences).[22] The results are shown in Figure 6B. Compared to an obvious decrease of impedance value of dsDNA/SPAN-GNO/CPE, the decrease of impedance value after hybridization with single-base mismatched sequences is small. When the ssDNA/SPAN-GNO/CPE was hybridized with ncDNA, the impedance value changed less than that obtained from the hybridization with single-base mismatched sequences. It can be seen that this DNA biosensor presents good selectivity for the DNA hybridization detection.[22,36]

Figure 6C shows the Bode plots obtained on the ssDNA/SPAN-GNO/CPE and hybridized with different concentrations of PML/RARA fusion gene sequence.[36] The difference (namely $\Delta\log Z$) between the log Z value of ssDNA/SPAN-GNO/CPE and that of the hybridization resulting electrode (dsDNA/SPAN-GNO/CPE) was selected as the measurement signal. The results show that the $\Delta\log Z$ value is linear with the logarithm of the concentrations of PML/RARA fusion gene sequence ranged from 1.0×10^{-7} mol/L to 1.0×10^{-13} mol/L. The regression equation is $\Delta\log Z = -0.128\log C - 1.8606$ and the regression coefficient (γ) is 0.9918 (Figure 6D). The detection limit is 3.2×10^{-14} mol/L using 3σ (where σ was the standard deviation of the blank solution, $n = 11$).[32]

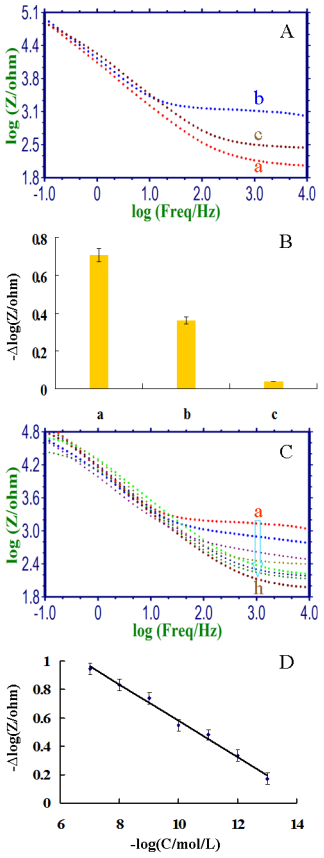

Figure 6. (A) Bode plots recorded at (a) SPAN-GNO/CPE, (b) ssDNA/SPAN-GNO/CPE, and (c) dsDNA/SPAN-GNO/CPE in 0.30 mol/L PBS (pH 7.0). (B) Histogram for comparison of signal change induced by hybridization: hybridized with (a) cDNA, (b) single-base mismatched DNA, and (c) ncDNA. Note: $\Delta\log(Z/\text{ohm}) = \log(Z_{\text{dsDNA}}) - \log(Z_{\text{ssDNA}})$. (C) Bode plots recorded at (a) ssDNA/SPAN-GNO/CPE and (b–h) after hybridization reaction with different concentrations of PML/RARA fusion gene sequence: (b) 1.0×10^{-13} mol/L, to (h) 1.0×10^{-7} mol/L in 0.30 mol/L PBS (pH 7.0). (D) Plot of $-\Delta\log Z$ vs. the negative logarithm of PML/RARA fusion gene sequence concentrations. Each point is the mean of three measurements, and the error bars correspond to the standard deviation.

CONCLUSION

In summary, a simple and economical approach to construct a novel direct DNA sensing platform based on highly conductive SPAN-GNO layers was developed. The SPAN-GNO layers presented good self-redox activity even in a neutral buffer (0.3 mol/L PBS, pH 7.0). Because of the existence of rich sulfonic acid groups of the SPAN-GNO layers, pDNA could be easily and firmly grafted on it via covalent binding. The SPAN-GNO layers suffered from the changes of conformation, electroconductivity, and so on, induced by DNA immobilization and hybridization. These changes can be easily detected by the sensitive EIS technique. The sensing platform does not require any complex labeling steps or any outer indicators, which endows it with simplicity, low cost, and noninvasiveness.

AUTHOR INFORMATION

Corresponding Author

*E-mail: taoyang@qust.edu.cn. Phone: +86-532-84022858. Fax: +86-532-84023927.

Notes

The authors declare no competing financial interest.

ACKNOWLEDGMENTS

This work was supported by the National Natural Science Foundation of China (21275084, 20975057), Doctoral Foundation of the Ministry of Education of China (20113719130001), Outstanding Adult-Young Scientific Research Encouraging Foundation of Shandong Province (BS2012CL013), and Scientific and Technical Development Project of Qingdao (12-1-4-3-(23)-jch).

REFERENCES

(1) Yan, L.; Zheng, Y. B.; Zhao, F.; Li, S. J.; Gao, X. F.; Xu, B. Q.; Weiss, P. S.; Zhao, Y. L. *Chem. Soc. Rev.* **2012**, *41*, 97–114.
(2) Huang, X.; Qi, X. Y.; Boey, F.; Zhang, H. *Chem. Soc. Rev.* **2012**, *41*, 666–686.
(3) Nardecchia, S.; Carriazo, D.; Ferrer, M. L.; Gutiérrez, M. C.; Monte, F. *Chem. Soc. Rev.* **2013**, *42*, 794–830.
(4) Yang, N. L.; Zhai, J.; Wan, M. X.; Wang, D.; Jiang, L. *Synth. Met.* **2010**, *160*, 1617–1622.
(5) Yan, X. B.; Chen, J. T.; Yang, J.; Xue, Q. J.; Miele, P. *ACS Appl. Mater. Interfaces* **2010**, *2*, 2521–2529.
(6) Wang, H. L.; Hao, Q. L.; Yang, X. J.; Lu, L. D.; Wang, X. *ACS Appl. Mater. Interfaces* **2010**, *2*, 821–828.
(7) Lu, J. L.; Liu, W. S.; Ling, H.; Kong, J. H.; Ding, G. Q.; Zhou, D.; Lu, X. H. *RSC Adv.* **2012**, *2*, 10537–10543.
(8) Bai, H.; Xu, Y. X.; Zhao, L.; Li, C.; Shi, G. Q. *Chem. Commun.* **2009**, 1667–1669.
(9) Peng, H.; Zhang, L.; Soeller, C.; Travas-Sejdic, J. *Biomaterials* **2009**, *30*, 2132–2148.
(10) Li, D.; Song, S. P.; Fan, C. H. *Acc. Chem. Res.* **2010**, *43*, 631–641.
(11) Chen, C. P.; Ganguly, A.; Wang, C. H.; Hsu, C. W.; Chattopadhyay, S.; Hsu, Y. K.; Chang, Y. C.; Chen, K. H.; Chen, L. C. *Anal. Chem.* **2009**, *81*, 36–42.
(12) Shrestha, S.; Yeung, C. M. Y.; Mills, C. E.; Lewington, J.; Tsang, S. C. *Angew. Chem., Int. Ed.* **2007**, *46*, 3855–3859.
(13) Hatchett, D. W.; Josowicz, M. *Chem. Rev.* **2008**, *108*, 746–769.
(14) Ghanbari, K.; Bathaie, S. Z.; Mousavi, M. F. *Biosens. Bioelectron.* **2008**, *23*, 1825–1831.
(15) Pham, M. C.; Piro, B.; Tran, L. D.; Ledoan, T.; Dao, L. H. *Anal. Chem.* **2003**, *75*, 6748–6752.
(16) Reisberg, S.; Piro, B.; Noël, V.; Pham, M. C. *Anal. Chem.* **2005**, *77*, 3351–3356.
(17) Arora, K.; Prabhakar, N.; Chand, S.; Malhotra, B. D. *Anal. Chem.* **2007**, *79*, 6152–6158.
(18) Dhand, C.; Das, M.; Datta, M.; Malhotra, B. D. *Biosens. Bioelectron.* **2011**, *26*, 2811–2821.
(19) Ma, Y. F.; Chiu, P. L.; Serrano, A.; Ali, S. R.; Chen, A. M.; He, H. X. J. *Am. Chem. Soc.* **2008**, *130*, 7921–7928.
(20) Hu, Y. W.; Yang, T.; Li, Q. H.; Guan, Q.; Jiao, K. *Analyst* **2013**, *138*, 1067–1074.
(21) Yang, T.; Guan, Q.; Li, Q. H.; Meng, L.; Wang, L. L.; Liu, C. X.; Jiao, K. *J. Mater. Chem. B* **2013**, *1*, 2926–2933.
(22) Hu, Y. W.; Yang, T.; Wang, X. X.; Jiao, K. *Chem.—Eur. J.* **2010**, *16*, 1992–1999.
(23) Yang, T.; Guan, Q.; Guo, X. H.; Meng, L.; Du, M.; Jiao, K. *Anal. Chem.* **2013**, *85*, 1358–1366.
(24) Yang, T.; Li, X.; Li, Q. H.; Guo, X. H.; Guan, Q.; Jiao, K. *Polym. Chem.* **2013**, *4*, 1228–1234.
(25) Du, M.; Yang, T.; Jiao, K. *J. Mater. Chem.* **2010**, *20*, 9253–9260.
(26) Li, G. C.; Zhang, C. Q.; Peng, H. R.; Chen, K. Z.; Zhang, Z. K. *Macromol. Rapid Comm.* **2008**, *29*, 1954–1958.
(27) Chen, J. H.; Zhang, J.; Wang, K.; Lin, X. H.; Huang, L. Y.; Chen, G. N. *Anal. Chem.* **2008**, *80*, 8028–8034.
(28) Zhou, M.; Wang, Y. L.; Zhai, Y. M.; Zhai, J. F.; Ren, W.; Wang, F.; Dong, S. J. *Chem.—Eur. J.* **2009**, *15*, 6116–6120.

(29) Zhang, C. Q.; Li, G. C.; Peng, H. R. *Mater. Lett.* **2009**, *63*, 592−594.
(30) Zhang, K.; Zhang, L. L.; Zhao, X. S.; Wu, J. S. *Chem. Mater.* **2010**, *22*, 1392−1401.
(31) Chen, G. L.; Shau, S. M.; Juang, T. Y.; Lee, R. H.; Chen, C. P.; Suen, S. Y.; Jeng, R. J. *Langmuir* **2011**, *27*, 14563−14569.
(32) Yang, T.; Li, Q. H.; Meng, L.; Wang, X. H.; Chen, W. W.; Jiao, K. *ACS Appl. Mater. Interfaces* **2013**, *5*, 3495−3499.
(33) Hu, Y. W.; Li, F. H.; Bai, X. X.; Li, D.; Hua, S. C.; Wang, K. K.; Niu, L. *Chem. Commun.* **2011**, *47*, 1743−1745.
(34) Meziane, D.; Barras, A.; Kromka, A.; Houdkova, J.; Boukherroub, R.; Szunerits, S. *Anal. Chem.* **2012**, *84*, 194−200.
(35) Zhang, W.; Yang, T.; Jiao, K. *Biosens. Bioelectron.* **2012**, *31*, 182−189.
(36) Yang, T.; Li, Q. H.; Li, X.; Du, M.; Jiao, K. *Biosens. Bioelectron.* **2013**, *42*, 415−418.